

ISOGI-Q Based Control Algorithm for Single Stage Grid Tied SPV System

Bhim Singh, *Fellow, IEEE*, Priyank Shah and Ikhlaz Hussain, *Member, IEEE*

Dept. of Electrical Engineering, Indian Institute of Technology Delhi, Hauz-Khas, New Delhi-110016, India

(p4priyank1504@gmail.com, ikhlaqb@gmail.com and bhimsinghiitd60@gmail.com)

Abstract- This paper deals with a single stage solar photovoltaic (SPV) array tied with a three phase grid by using an improved second order generalized integrator quadrature signal generator (ISOGI-QSG) based control algorithm to improve power quality of the grid. The maximum point power tracking (MPPT) is achieved by using an incremental conductance method. The incremental conductance MPPT method is effective to extract maximum power from a SPV array as well as to regulate the DC link voltage. ISOGI-QSG based control algorithm is robust and enhances the power quality in terms of load balancing, noise elimination and power factor correction (PFC) very effectively. Having D-STATCOM capabilities of SPV based system is useful to supply the active power to grid as well as to loads. The control algorithm is verified on proposed system topology and obtained responses are found satisfactory and total harmonic distortion (THD) of source currents within standard limit.

Keywords- D-STATCOM; ISOGI-QSG; MPPT; Power Quality and SPV.

I. INTRODUCTION

Nowadays the use of solar power generation is booming because of increased research on SPV, manufacturing technologies, rolling down price of SPV generation, new government policies and subsidy. However, conventional sources are main reason for warming on the planet and having threat to the environment by using highly carbon intensive fuel like coal to keep energy economical [1-2]. Moreover, SPV based system is having advantage of fast installation, eco-friendly and clean energy. Nowadays, photovoltaic (PV) system is used in residential, agriculture, telecommunication; healthcare services etc. Moreover, the power quality of the grid is degraded due to non-linear loads like variable frequency drives (VFD), switch mode power supply (SMPS), arc furnace etc in the distribution network at point of common coupling (PCC).

The second order generalized integrator (SOGI) based control algorithm is introduced by Yada et al. [3] for shunt active power capabilities for a three phase four wire grid connected system. The SOGI based structure has lower filtering capabilities and higher calculation time. Second order generalized integrator– quadrature (SOGI-Q) based control algorithm for double stage solar energy conversation system (SCES) integrated with three phase grid for multifunctional purpose is introduced by Jain et al. [4]. SOGI-Q based structure has worst attenuation around center frequency. The

SRF-PLL based control algorithm is introduced by Tripathi et al. [5] for double stage SPV based grid connected system. Double frequency oscillations problem is encountered in SRF based PLL structure.

Many techniques are introduced to implement PV model by Villalva et al. [6]. Many MPPT methods like differentiation technique, current compensation method, forced oscillation technique, look-up table method, perturb and observe method, load voltage maximization are available to extract maximum power point from SPV in literatures [7-8]. The reference voltage is obtained from MPPT and it is used further to maintain DC link voltage by (PI) controller tuning. The power loss comparison for single stage and two stage grid-connected PV systems is introduced by Wu et al. [9]. It is also mentioned that if the voltage range is properly chosen then a single stage has high efficiency, low cost and reducible size compared to a two stage grid connected SPV based system. An improved dual second order generalized integrator-quadrature signal generator based structure is introduced by Li et al. [10] for grid synchronization under non-ideal grid voltage including DC offset.

The proposed system consists of a single stage topology of a SPV based system having D-STATCOM (distribution static compensator) capabilities interfaced to the grid to meet power quality improvement like power factor correction, load balancing and harmonics mitigation. The ISOGI-QSG based control algorithm has advantage of being less sensitive toward input DC signal and other sub-harmonic. The control algorithm is very effective to estimate reference grid current without loss of accuracy. To confirm viability of control algorithm, experiments are performed on a developed hardware in the laboratory for various conditions like reactive power compensation, variable solar insolation, load unbalancing at load side network.

II. PROPOSED SYSTEM CONFIGURATION

The proposed system architecture consists of a three phase grid, SPV array system, ripple filter, DC link capacitor, voltage source converter (VSC) and non-linear loads. Fig. 1 shows the proposed topology to validate the control algorithm. The proposed system is implemented for three phase grid tied with a

single stage SPV based system. The proposed system parameters are designed as per procedure reported in [11-12].

III. CONTROL ALGORITHM

The ISOGI-QSG based control algorithm is used to estimate quadrature component of fundamental load current. An incremental conductance MPPT method is used here to get maximum power point to operate SPV array at MPPT point. This control algorithm is used also to mitigate power quality problems. Fig. 2 shows the overall control algorithm.

A. MPPT Control

An incremental conductance MPPT method is used here to get operating point for a SPV array. The voltage and current are sensed and used to estimate the difference between successive measurements of as following.

$$\frac{dP}{dV} = 0 \quad (1)$$

$$\frac{d(VI)}{dV} = I + V \frac{dI}{dV} = 0 \quad (2)$$

$$-\frac{I}{V} = \frac{dI}{dV} \quad (3)$$

In above equation, left hand side represents an incremental conductance and right hand side represent SPV array's instantaneous conductance. It is expressed under different operating condition as,

$$-\frac{I}{V} = \frac{dI}{dV} \left(\frac{dP}{dV} = 0 \right) \quad (4)$$

$$-\frac{I}{V} > \frac{dI}{dV} \left(\frac{dP}{dV} < 0 \right) \quad (5)$$

$$-\frac{I}{V} < \frac{dI}{dV} \left(\frac{dP}{dV} > 0 \right) \quad (6)$$

Above equation is used to decide direction of perturbation to reach MPP point of SPV array. Whenever MPPT point is achieved then a change in current remains constant. Whenever,

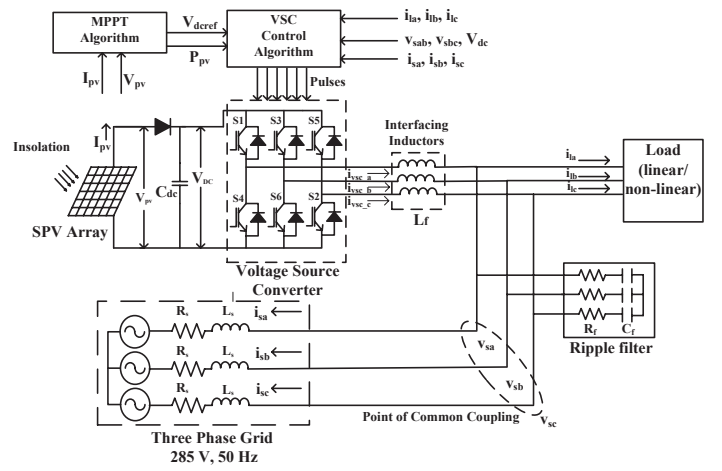


Fig. 1 The schematic diagram of proposed system topology. climate condition changes then a new MPP is tracked by an incremental conductance. This MPPT generates the reference DC link voltage for control of VSC.

B. Switching Control of VSC

The switching control algorithm includes the estimation amplitude of terminal voltage of common coupling point (CCP), estimation of in-phase unit templates, PV feed forward term, loss component and reference current estimation for grid currents. Fig. 2 shows the overall architecture for control algorithm.

The amplitude of terminal voltage (V_t) of CCP is evaluated by sensing line voltages (v_{sab} and v_{sbc}). From sensed two line voltages, phase voltages are obtained as,

$$\begin{bmatrix} v_{sa} \\ v_{sb} \\ v_{sc} \end{bmatrix} = \frac{1}{3} \begin{bmatrix} 2 & 1 & 0 \\ -1 & 1 & 0 \\ -1 & -2 & 0 \end{bmatrix} \begin{bmatrix} v_{sab} \\ v_{sbc} \\ 0 \end{bmatrix} \quad (7)$$

The amplitude of terminal voltage (V_t) is obtained as,

$$V_t = \sqrt{\frac{2}{3}(v_{sa}^2 + v_{sb}^2 + v_{sc}^2)} \quad (8)$$

The in-phase unit templates (u_a , u_b and u_c) are evaluated by using the amplitude of terminal voltage and phase voltages as,

$$u_a = \frac{v_{sa}}{V_t}, u_b = \frac{v_{sb}}{V_t}, u_c = \frac{v_{sc}}{V_t} \quad (9)$$

The ISOGI-QSG based control method used here to extract the quadrature component of fundamental from load current which is highly distorted due to non-linear loads in the distribution network. Fig. 3 shows a structure of ISOGI-QSG based control. The in-phase component (i_v) and quadrature component (i_{qv}) of fundamental of load current are shown in Fig. 3. The transfer function of ISOGI-QSG is given as,

$$\frac{i_{v'}(s)}{i(s)} = \frac{k_{sq} \times \omega \times s^2}{\Delta(s)} \quad (10)$$

$$\frac{i_{qv'}(s)}{i(s)} = \frac{k_{sq} \times \omega^2 \times s}{\Delta(s)} \quad (11)$$

$$\frac{i_{DC}(s)}{i(s)} = \frac{k_{DC} \times \omega \times (s^2 + \omega^2)}{\Delta(s)} \quad (12)$$

Where, $\Delta(S) = S^3 + (k_{sq} + k_{DC})\omega s^2 + \omega^2 s + k_{DC}\omega^3$, k_{sq} and k_{DC} are needed to tune with help of Routh-Hurwitz stability criteria. The parameter k_{DC} is opted base on $\Delta(s)$. All roots of $\Delta(s)$ must have equal real part.

Then k_{DC} must fulfill the condition as [10],

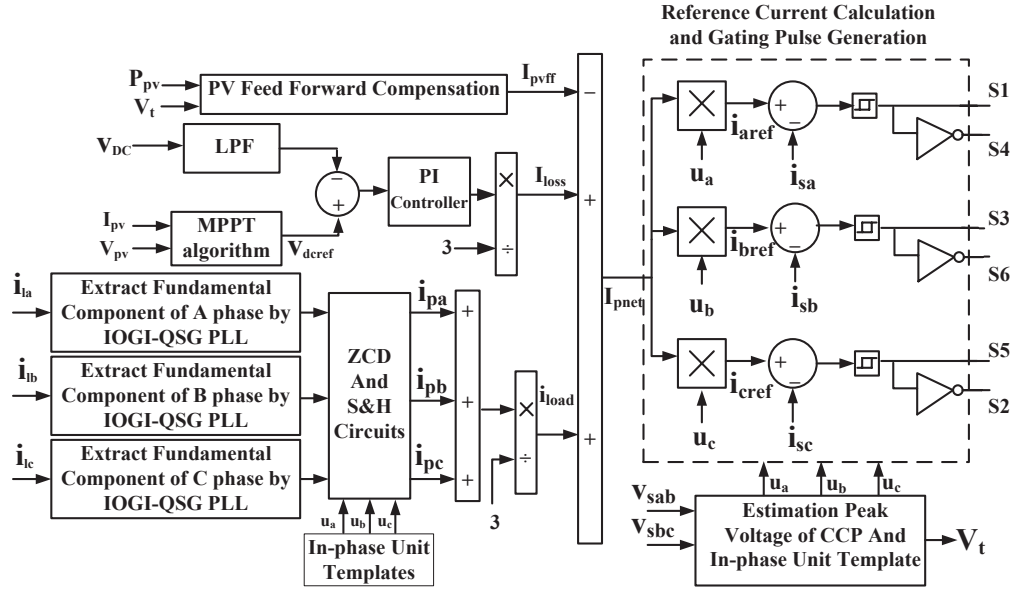


Fig. 2 Block diagram of control algorithm.

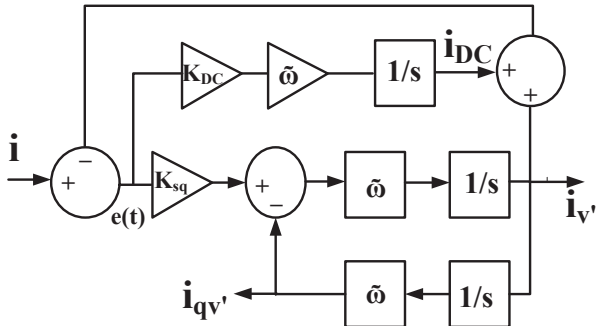


Fig. 3 Block Diagram of ISOGI-QSG.

$$k_{DC}^3 + 3k_{sq}k_{DC}^2 + (3k_{sq}^2 + 9)k_{DC} + k_{sq}^2 - 4.5k_{sq} = 0 \quad (13)$$

The ISOGI-QSG has high capacity to eliminate the DC offset from input signal by estimating it from error $e(t)$ and added back to feed-back path. The amplitude of quadrature component for three phases (i_{ap} , i_{bp} and i_{cp}) is obtained by using unit templates, sample and hold circuit respectively. From that amplitude, net weight of load component (I_{load}) is evaluated as,

$$I_{load} = \frac{i_{ap} + i_{bp} + i_{cp}}{3} \quad (14)$$

The PV feed forward term is calculated by using SPV array power and it is estimated for phase. Therefore PV feed forward (I_{pvff}) is evaluated as,

$$I_{pv} = \frac{2P_{pv}}{3V_t} \quad (15)$$

The loss component is calculated by using reference DC link voltage obtained from MPPT and sensed VSC-DC link capacitor voltage. So loss component (I_{loss}) is evaluated as,

$$I_{loss} = \frac{1}{3}(V_{dcref} - V_{dc})(k_p + \frac{k_f}{s}) \quad (16)$$

The reference source currents are estimated by using in-phase templates (u_a , u_b and u_c) and net weight (I_{net}). The net weight (I_{net}) is obtained from load active current component (i_{ap} , i_{bp} and i_{cp}) and SPV feed forward term (I_{pvff}) and loss component (I_{loss}). The reference currents are calculated as,

$$I_{net} = I_{load} - I_{pvff} + I_{loss} \quad (17)$$

$$i_{aref} = u_a \times I_{net} \quad (18)$$

$$i_{bref} = u_b \times I_{net} \quad (19)$$

$$i_{cref} = u_c \times I_{net} \quad (20)$$

The error between source current (i_{sa} , i_{sb} and i_{sc}) and estimated source current (i_{aref} , i_{bref} and i_{cref}) are passed through hysteresis controller and generate switching pulses for VSC.

IV. EXPERIMENTAL RESULTS

This section shows the experimental results of proposed system topology to validate ISOGI-QSG based control algorithm. The SPV simulator (AMTECH ETS600×17DPVF) is used as SPV array. The ISOGI-QSG based control algorithm is implemented by a real time controller (DSPACE-1202). The voltages of CCP are sensed by voltage sensors (LV25-P) and source currents are sensed by current sensors (LA55-P). The dynamics of proposed system is observed by digital scope (AGILENT DSO 7014A) and steady state response of proposed topology is observed by power analyzer (Fluke-43B). The control algorithm is demonstrated here for various conditions.

A. Steady State Response of the System Under Linear Load

Fig. 4 shows the steady state response of the proposed system under a linear load. Figs. 4 (a-b-c) show v_{sab} with i_{sa} , i_{la} , and i_{vsc_a} respectively. Fig. 4 (d) shows load power (1.94kVA) at poor power factor (PF=0.72). Fig 4 (e) shows the improvement of power factor of the distribution network to unity. Moreover, the reactive power compensation is achieved by SPV coupled VSC based topology. Fig. 4 (f) shows SPV power (P_{pv}). The SPV array coupled VSC based topology supplies an active power and the reactive power to the distribution network and the load.

B. Steady State Response of System Under Non linear Load

Fig. 5 shows the steady state response of the single stage grid connected SPV system. In this Fig. 5, the waveforms of grid voltage (v_{sab}), grid current (i_{sa}), load current (i_{la}) and VSC current (i_{vsc_a}) are shown. Figs. 6 (a-b-c) show the waveforms of grid voltage (v_{sab}) and grid current (i_{sa}), v_{sab} and load current (i_{la}), v_{sab} and VSC current (i_{vsc_a}) respectively. Fig 6 (d) shows that THD of grid current (i_{sa}) which is 3.4%. It follows IEEE-519 standard [13]. Figs.6 (e-f) show that THD of

grid voltage is 1.5% and load current has THD of 27.5%. From Figs. 6 (h-i-j) show that SPV array power not only supplies to the load but it also supplies to grid by improving power quality of the grid.

C. Dynamic Response of System under Unbalancing

Fig. 7 shows the dynamic response of the system under unbalancing condition. Fig. 7 (a) shows the error $e(t)$,

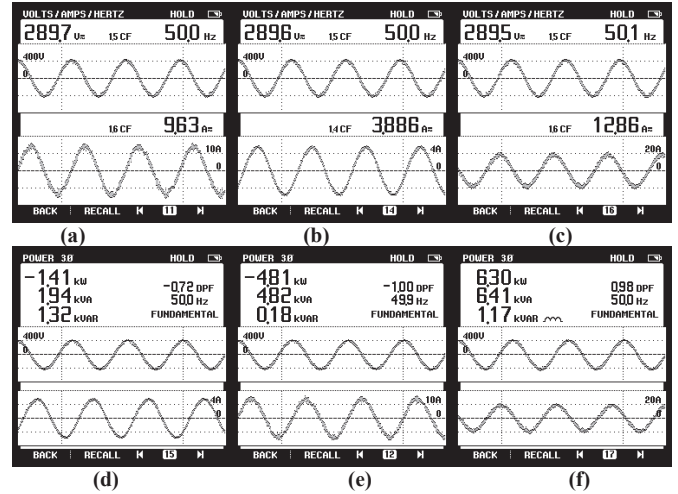


Fig. 4 Steady state response of system under linear load (a) v_{sab} and i_{sa} (b) v_{sab} and i_{la} (c) v_{sab} and i_{vsc_a} (d) load power and load power factor (e) grid power and source power factor (f) SPV-VSC power

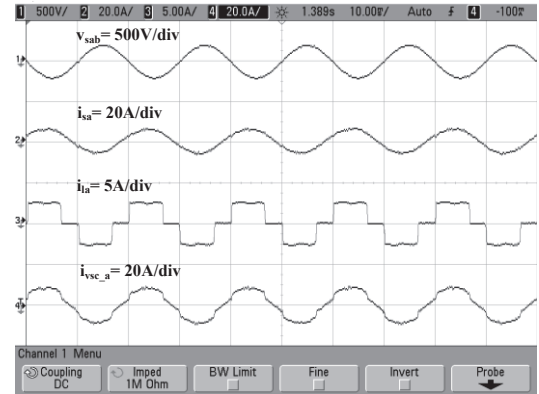
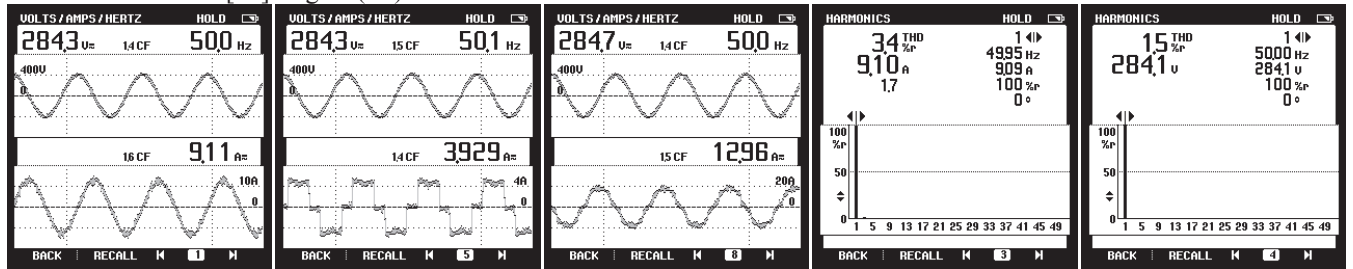


Fig. 5 Steady state response of system under nonlinear load



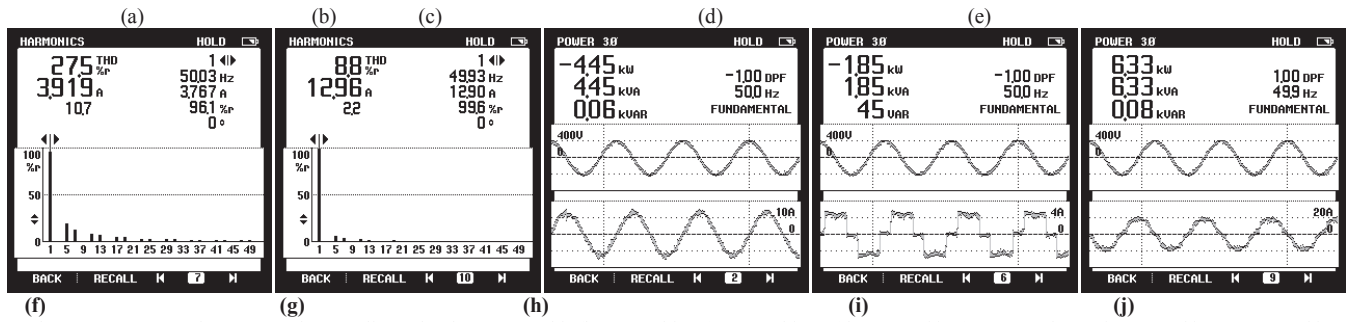


Fig. 6 Steady state response of system under non-linear load (a) v_{sab} and i_{sa} (b) v_{sab} and i_{la} (c) v_{sab} and i_{vsc_a} (d) THD of i_{sa} (e) THD of v_{sab} (f) THD of i_{la} (g) THD of i_{vsc_a} (h) grid power (i) load power (j) SPV-VSC power.

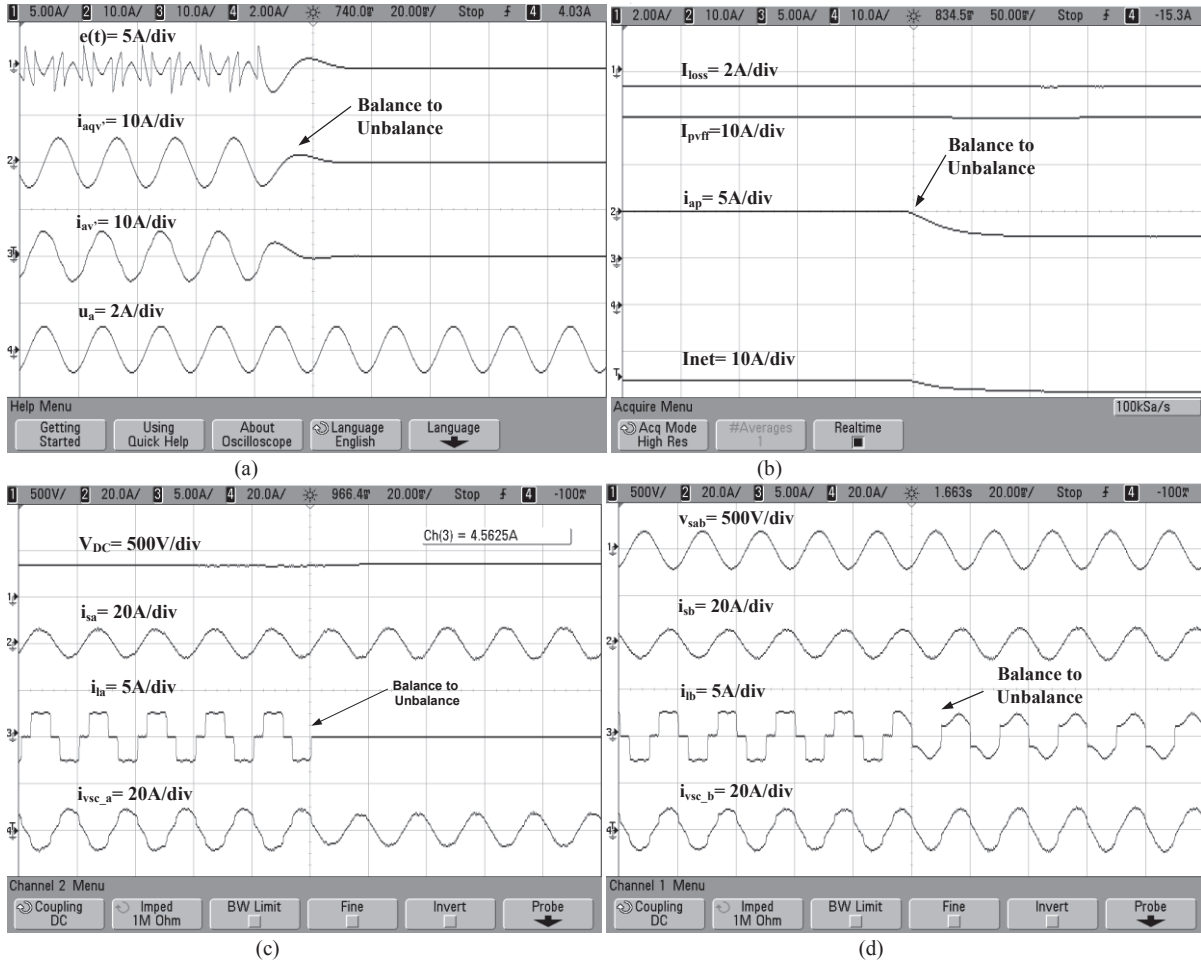


Fig. 7 Dynamic response of system under unbalancing (a) $e(t)$, i_{aqv} , i_{av} and u_a (b) I_{loss} , I_{pvff} , i_{ap} and I_{net} (c) V_{DC} , i_{sa} , i_{la} and i_{vsc_a} (d) v_{sab} , i_{sb} , i_{lb} and i_{vsc_b} .

quadrature and in-phase component of fundamental load current (i_{aqv} and i_{av}) and unit template (u_a) under unbalancing occurred in A phase. Fig. 7 (b) shows the loss component (I_{loss}), PV feed forward term (I_{pvff}), fundamental amplitude of A phase load current (i_{ap}) and net weight (I_{net}). Fig. 7 (c) shows dynamics of DC link voltage (V_{DC}), grid current (i_{sa}), load current (i_{la}) and compensating current (i_{vsc_a})

respectively for A phase during unbalancing under non-linear load. Fig. 7 (d) shows the of DC link voltage (V_{DC}), grid current (i_{sb}), load current (i_{lb}) and VSC current (i_{vsc_b}) respectively for B phase during unbalancing of A phase.

D. Dynamic Response of System under Variable Solar Insolation

Figs. 8 and 9 show the dynamic response of the system under variable solar insolation. Figs.8(a-b) show solar insolation of a SPV simulator changed from 700 to 1000 W/m². As solar insolation increase, SPV array current as well as grid current is also increased. Fig. 9 (a) shows the loss component (I_{loss}), PV feed forward component (I_{pvff}), amplitude of fundamental component of load current (i_{ap}) and net weight (I_{net}). Fig. 9 (b) shows the dynamics of V_{DC} , SPV array current (I_{pv}), VSC current (i_{vsc_a}) and grid current (i_{sa}).

V. CONCLUSION

A three phase single stage grid connected SPV based system having has demonstrated reactive power compensation capabilities by using ISOGI-QSG based control algorithm to

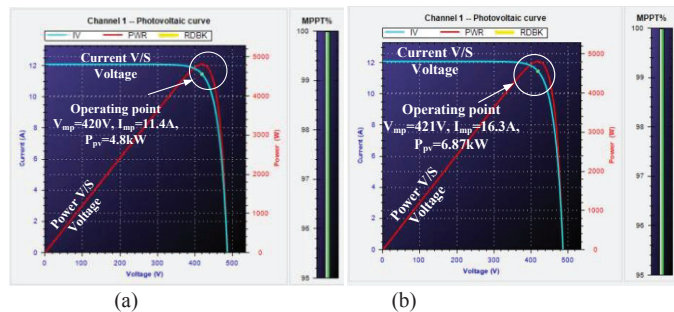


Fig.8 Solar insolation increase (a) 700W/m² (b) 1000W/m².

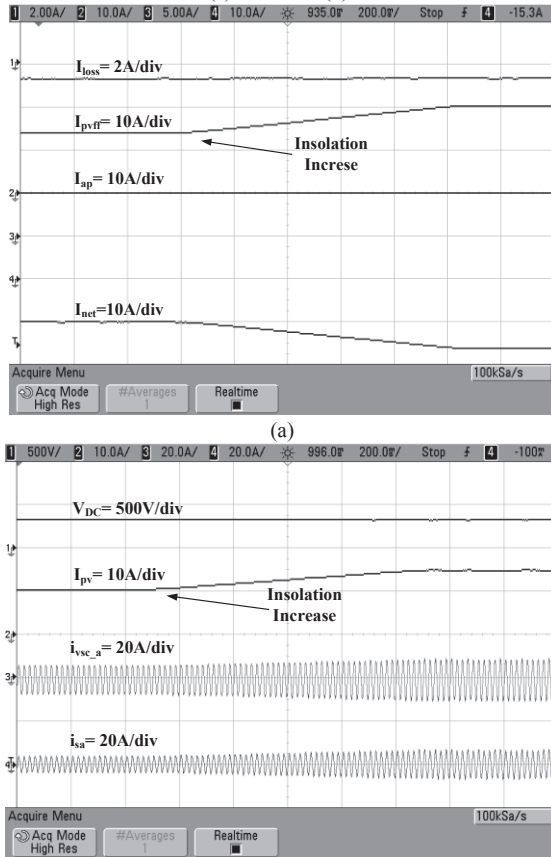


Fig. 9 Response of system under variable solar insolation, (a) I_{loss} , I_{pvff} , I_{ap} and I_{net} (b) V_{DC} , I_{pv} , i_{vsc_a} and i_{sa} .

improve power quality like power factor correction (PFC), harmonics elimination and load balancing at distribution network. The ISOGI-QSG based structure has more DC signal filtering capability and good attenuate around central frequency compared. The THD of source currents are found within the limit according to an IEEE-519 standard. Experimental results have showed that ISOGI-QSG based control algorithm works satisfactory and robust during various conditions like reactive power compensation, variable solar insolation and load unbalancing.

APPENDICES

Experimental parameters: SPV array simulator $V_{mp}=421V$, $I_{mp}=16.3A$, $P_{pv}=6.87kW$; DC link voltage= 421 V; converter rating= 25 kVA; ripple filter $R_f=5\Omega$, $C_f=10\mu F$; Interfacing inductor $L_f=2.9mH$; $k_{sq}=1.41$; $k_{DC}=0.22$; source voltage $v_{sab}=285V$, 50 Hz; non-linear load=1.85 kVA, linear load= 1.94 kVA; $k_p=0.14$, $k_i=0.001$; sampling time $T_s=30\mu s$.

ACKNOWLEDGMENTS

Authors are highly thankful to DST, Govt. of India, for supporting this project under Grant Number: RP02583.

REFERENCES

- [1] L. Suganthi and A. Williams, "Renewable energy in India- a modeling study for 2020-2021," *Energy Policy*, vol. 28, no. 15, pp.1095-1109, Dec 2000.
- [2] A. Ashwin Kumar, "A study on renewable energy resources in India," in *Proc. International Conf. on Environmental Engineering and Applications*, pp.49-53, 10-12 Sept 2010.
- [3] H. K. Yada and M. S.R. Murthy, "A new topology and control strategy for extraction of reference current using single phase SOGI-PLL for three phase four-wire with shunt active power filter," in *Proc. IEEE Conf. Power Electron., Drive Energy System (PEDES)*, pp. 1-6, 19-19 Dec, 2014.
- [4] Chinmay Jain and Bhim Singh, "A SOGI-Q based control algorithm for multifunctional grid connected SECS," in *Proc. IEEE 6th India International Conf. Power Electronics (IICPE)*, pp. 1-6, 8-10 Dec. 2014.
- [5] R.N. Tripathi and A. Singh, "SRF theory based interconnected solar photovoltaic (SPV) system with improved power quality," in *Proc. IEEE Emerging Trends In Communication, Control, Signal Processing & Computing Application*, pp. 1-6, 10-11 Oct. 2013.
- [6] M. Gradella Villalva, Jonas Rafael Gazoli and Ernesto Ruppert Filho, "Comprehensive Approach to Modeling and Simulation of Photovoltaic Arrays," *IEEE Trans. on Power Electronics*, vol.24, No. 5, May 2009.
- [7] Anup Anurag, S. Bal, S. Sourav and M. Nanda, "A review of maximum power point tracking techniques for photovoltaic systems" *International Journal of Sustainable Energy*, vol.35, No. 5, 19 May 2014.
- [8] M. E. El Telbany, A. Youssef and A. A. Zerky, "Intelligent techniques for MPPT control in photovoltaic systems: A comprehensive review," in *Proc. 4th International Artificial Intelligence with Application Engineering and Technology*, pp.17-22, 3-5 Dec, 2014.
- [9] Tsai-Fu Wu, Chih-Hao Chang, Li-Chuin Lin and Chia-Ling Kuo, "Power loss comparison of single and two stage grid-connected photovoltaic systems" *IEEE Transaction on Energy Conversion*, vol. 26, no. 2, pp.707-715, June. 2011.

- [10] J. Li, J. Zhao, J. Qu and Ping-ping Xu, "Improved dual second order generalized integrator PLL for grid synchronization under non-ideal grid voltages including DC offset" in *Proc.IEEE Energy Conservation Congress Exposition (ECCE)*, pp.136-141, 14-18 Sept 2014.
- [11] B. Singh, A. Chandra and K. Al-Haddad, *Power quality: problems and mitigation techniques*, John Wiley & Sons Ltd., United Kingdom, 2015.
- [12] R. Agrawal, I. Hussain and Bhim Singh, "LMF based control algorithm for single stage three phase grid integrated solar PV system" *IEEE Trans. Sus.Energy*, vol. 7, no. 4, pp. 1379-1387, Oct. 2016.
- [13] IEEE Recommended Practice and Requirement for Harmonic Control on Electric Power System, IEEE std. 519, 1992.